Dynamic Analysis of Crankcase and Crankshaft

Gouthami S. Tulasi, *Post Graduate Student, Department of Mechanical Engineering, RSCOE JSPM Pune*, S. M. Jadhao, *Assistant Professor, Department of Mechanical Engineering, RSCOE JSPM Pune*

***Abstract*—An agricultural single cylinder four stroke engine experienced failure at customer location. This had to be taken care of immediately as it had affected the engine sales. To investigate the reason for failure various conventional methods were employed which include static analysis, but as static analysis could not explain the appropriate cause, dynamic analysis was considered. The process was divided into two stages first being determination of gas force, inertia force, bending force and torsional force through extensive excel sheet calculations considering the engine to be a single degree of freedom slider-crank mechanism. The loads acting on the engine for varied crankshaft angles were thus determined. A plot of these loads was presented to define the characteristics of the engine. For stage two a unique methodology known as superposition theory has been implemented. This involved applying unit load for calculating stresses and then scaling them to the magnitude of applied loads. An extensive dynamic testing has been performed by placing strain gauges at locations of criticality. The objective of the paper is to evaluate the scaled stress values in comparison to the stress values determined through experimentation.**

***Index Terms*—crankcase, crankshaft, crankshaft angles dynamic analysis, force calculations, superposition theory, stress location**

I. INTRODUCTION

THE manufacturer and assembler of agricultural engines was facing failure of crankcase at customer location . The failure was due to crack initiation at the flywheel side in a fillet area, close to the main bearing cap. An earlier static analysis based on FEM confirmed the location of failure but the reason remained unclear. With motivation from earlier investigation this study intends to explore the reason through dynamic analytical calculations and experimentation. The crankshaft experiences a complex loading due to the motion of the connecting rod, which transforms two sources of loading to the crankshaft. The main objective of this study is to perform dynamic analysis of crankcase and crankshaft which requires accurate magnitude of the loading on these components that consists of bending and torsion. In addition, there is a need for obtaining the stress variation during a loading cycle and this requires FEA over the entire engine cycle. To obtain the forces acting on crankcase, first loading on crankshaft is considered which is treated as a simply supported beam and the reaction forces at the bearings of crankcase are calculated.

The analytical approach was solved for a general slider crank mechanism which results in equations that could be used for any crank radius, connecting rod geometry, and connecting rod mass, connecting rod inertia, engine speed, engine acceleration, piston diameter, piston and pin mass, pressure inside cylinder diagram, and any other variables of the engine. These equations are derived in Appendix I**.** The equations provided the values of velocity and acceleration of the piston and forces at the connecting rod crankshaft bearing [5]. It should be pointed out that in this analysis it was assumed that the crankshaft rotates at a constant angular velocity, which means the angular acceleration was not included in the analysis [4].

II. LITERATURE REVIEW

A crankcase failure incident was observed in an on-road endurance test of scooter engine by K. Sriram, R. Govindarajan, K. Nagaraja, Ravi Kharul and N. Jayaram of TVS motor company ltd [1]. To address the issue FEM techniques were applied to investigate the stress fields in the region of crack formation. The authors here considered unit static load acting in the stress fields due to unavailability of direct methods to evaluate actual dynamic load value. This condition is seen to be referred for subsequent calculations in our study. They created a solid Pro-E model meshed with tetrahedral elements and analyzed in ANSYS. The results showed stress contours coinciding with the region of crack formation which occurred during the static test and dynamometer crack test. The design was optimized by adding rib pattern to the crack initiation area which increased cracking resistance four times in comparison to the initial design. This was validated using dynamometer dynamic test. Similar approach was observed to strengthen crankcase given in our problem statement.

Alexandre Schalch Mendes, Emre Kanpolat and Ralf Rauschen [2] performed durability analysis considering conventional methodologies of dynamic simulations for the crankshaft and quasi-static simulations for the crankcase at the main bearings regions. These tests resulted in cracks at flywheel side in a fillet area close to the main bearing cap which were due to the bending vibrations of the crankshaft. As an adaptive solution a steel plate ladder was introduced at the bottom of the crankcase to increase the stiffness of the main bearings, thus reducing the stress amplitudes at the fillet area. Considering a simulated in-line 6 cylinder engine of 180 bar peak cylinder pressure a hybrid simulation was performed. The process was divided into two steps. Initial step computed the responses of the components to the excitation generated by the combustion and reciprocating masses through the elastic multi body simulation using *FEV Virtual Engine* and then the next step an implicit nonlinear FE model was used to calculate

the total stresses on the crankcase for a durability analysis using *fe-safe* tool. When a 430 hour engine test was performed at full load condition the crankcase, it showed failure in the test bed which coincided with the theoretical durability analysis-a part of full dynamic study for an engine without ladder frame. When the same full dynamic study was performed on a crankcase with ladder frame the fatigue design margin was seen to be elevated. Thus the study showed an effective usage of hybrid dynamic simulation to detect the fatigue crack issues and solve a crankcase-crankshaft coupled model with high accuracy. With reference to this research, dynamic study has been adopted to solve the crack initiation issue for the mentioned problem

Hiroshi Kuribara, Junya Saito, Hidei Saito, Daisuke Sekiya [3] predicted the possibility of crankcase failure initiating from root of internal thread due to fatigue fracture. So they developed a technology that uses FEM analysis to theoretically evaluate the fatigue strength of the entire crankcase, including the internal thread portions of the main bolts. A characteristic issue with aluminum crankcases is fatigue fracture in the engine starting from the roots of the internal threads of the fastening areas of bolts subject to high axial force, such as the cylinder head stud bolts and the crankshaft main bearing fastening bolts. Three processes were used to develop the technology, an FEM model for stress analysis of the bolt fastening area, an FEM model for entire crankcase stress analysis, and a method for calculating the fatigue safety factor. A dynamic verification of FEM stress values was performed using strain gauges placed carefully at locations referring to the strain distribution pattern obtained from FEM results. Comparing the actual measurements and FEM analysis results, a high correlation was confirmed both qualitatively and quantitatively, and the validity of the engine assembly FEM model was verified. The use of strain gauges to evaluate the results of the dynamic study is key in our experimentation.

Farzin H. Montazersadgh and Ali Fatemi [4] report on Stress Analysis and Optimization of Crankshafts Subjected to Dynamic Loading has formed framework for performing dynamic calculations on our crankcase-crankshaft as their work refers to a single cylinder four stroke engine similar to the one given in problem statement. They conducted dynamic simulation on two crankshafts, cast iron and forged steel, for similar single cylinder four stroke engines. Finite element analysis was performed to obtain the variation of stress magnitude at critical locations. The pressure-volume diagram was used to calculate the load boundary condition in dynamic simulation model, and other simulation inputs were taken from the engine specification chart. The dynamic analysis was done analytically and was verified by simulations in ADAMS. This load was then applied to the FE model in ABAQUS, and boundary conditions were applied according to the engine mounting conditions. The analysis was done for different engine speeds and as a result, critical engine speed and critical region on the crankshafts were obtained. Results from FE analysis were verified by strain gages attached to several locations on the forged steel crankshaft. The analysis and calculations performed on crankshaft in the above report have been applied to our crankcase and results have been validated through dynamic testing.

III. Dynamic Analysis for the Actual Crankshaft and Crankcase

The engine is a single cylinder four stroke diesel engine with power output of 8 HP. The pressure versus crank angle of this specific engine was not available, so the pressure versus crank angle diagram of a similar engine was considered. This diagram was scaled between the minimum and maximum of pressure and the crank angle. Figure 1 shows the pressure versus crankshaft angle, which was used as the applied force on the piston during the dynamic analysis. It should be noted that the pressure versus crank angle of the cylinder graph changes as a function of engine speed, but the changes are not significant and the maximum pressure which is the critical loading situation does not change. Therefore, the same diagram was used for different engine speeds in this study. The analytical results of the slider crank mechanism are linear velocity and acceleration of the piston assembly and forces that are being applied to the bearing between the crankshaft and the connecting rod. The values were determined for different engine speeds in the operating engine speed range.

Results from the analytical calculations obtained through Excel program with reference to Appendix I at the engine speed of 2600 are plotted in Figure 1 through Figure 6.

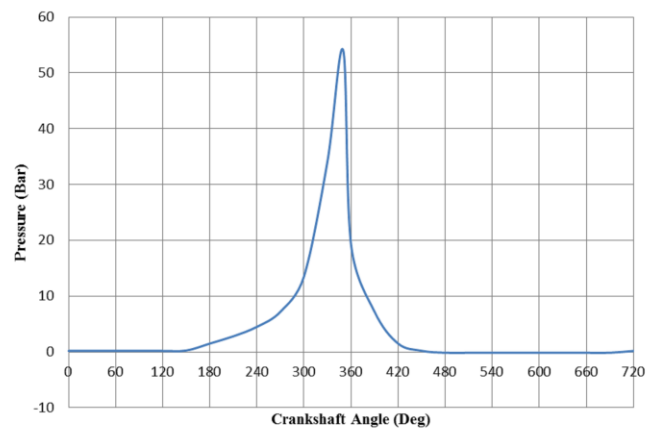

Figure 1. Pressure versus crankshaft angle used to calculate the forces at the surface of the piston

The position of piston during the complete cycle is shown in Figure 2. Figures 3 and 4 show the variation of linear velocity and linear acceleration of the piston assembly over 720 degrees, respectively. Note that variations of velocity and acceleration in piston assembly from 0° to 360° are identical to their variation from 360° to 720°. Figure 5 shows the forces generated during the complete cycle of an engine. P_G in Figure 5 is the force acting due to gas pressure whereas P_I is the force due to inertia of rotating crankshaft.

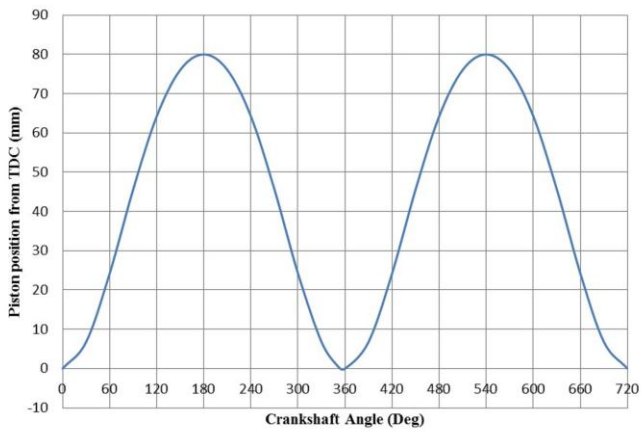

Figure 2. Piston position from TDC versus crankshaft angle

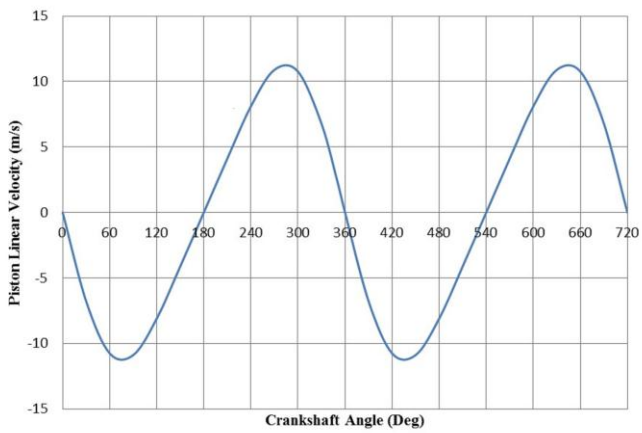

Figure 3. Variation of linear velocity of the piston assembly over one complete engine cycle at crankshaft speed of 2600 rpm

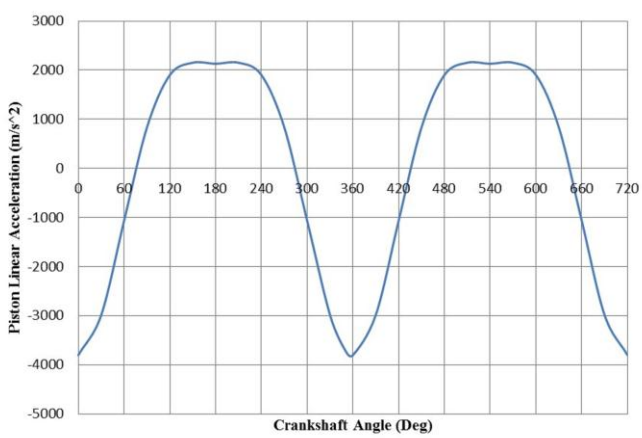

Figure 4. Variation of linear acceleration of the piston assembly over one complete engine cycle at crankshaft speed of 2600 rpm

The total force acting on crankpin is the summation of gas forces and inertial forces. This total force is resolved into two components bending and torsion which are acting on the crankpin. Figure 6 shows the variation of the force defined in the local/rotating coordinate system. F_x in Figure 6 is the force that causes bending during service life and F_y is the force that causes torsion on the crankshaft. As can be seen in this figure, the maximum loading happens at the angle of 350° where the combustion takes place. The variation of forces defined in the local coordinate system at 2000 rpm and 3000 rpm engine speeds are shown in Figures 7 and 8 respectively.

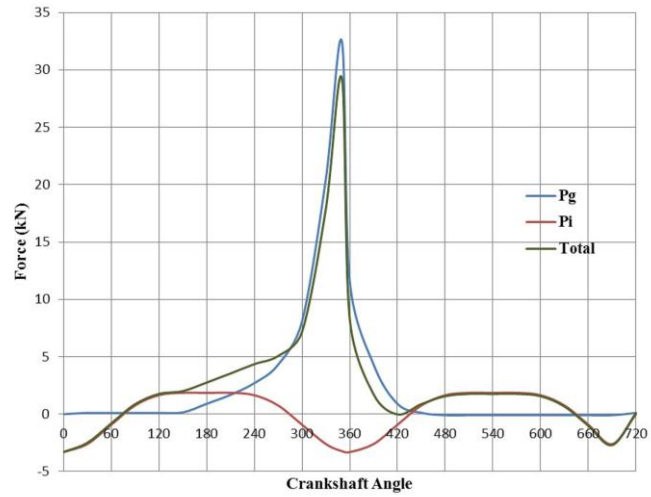

Figure 5. Variation of the Gas and Inertial forces over one complete cycle at the crank end of the connecting rod at 2600 rpm

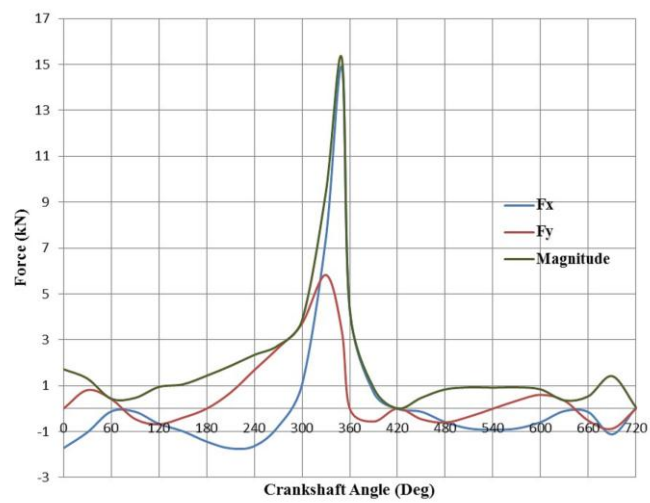

Figure 6. Variation of the force components over one complete cycle at the crank end of the connecting rod at 2600 rpm

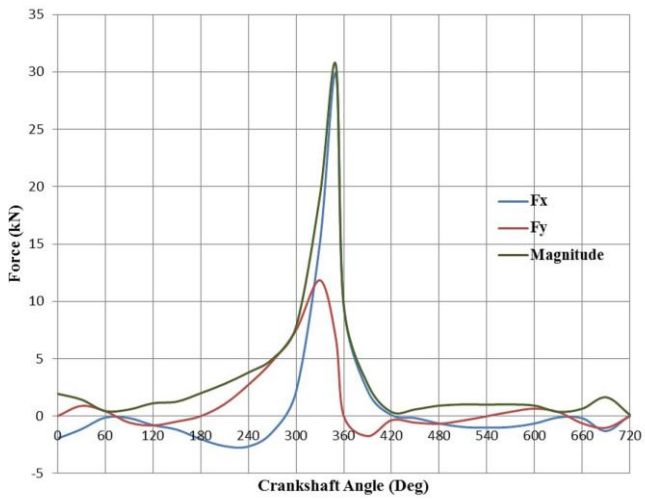

Figure 7. Variation of the force components over one complete cycle at the crank end of the connecting rod at 2000 rpm

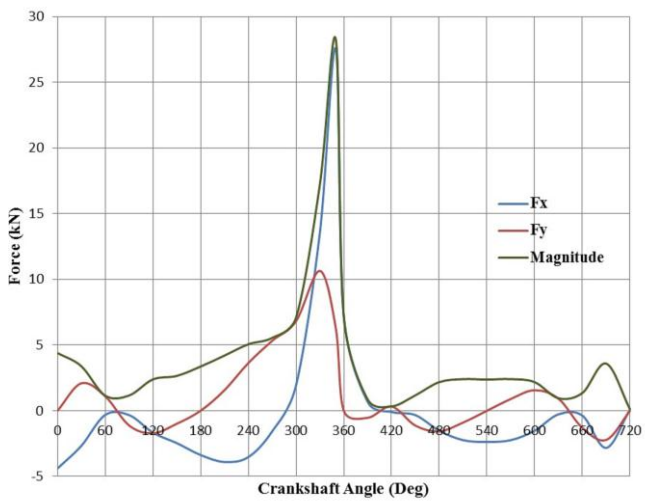

Figure 8. Variation of the force components over one complete cycle at the crank end of the connecting rod at 3000 rpm

Figure 9 compares the magnitude of maximum gas force, inertia force, torsional load and bending load at different engine speeds. Note from this figures that as the engine speed increases the maximum bending load decreases. As the engine speed increases the maximum bending load decreases. Since the maximum pressure in the cylinder does not change as the engine speed changes, hence the load applied at the crankshaft due to the maximum pressure due to combustion does not change. But the load caused by inertia changes. The load produced by combustion is greater than the load caused by inertia and is in the opposite direction, which means the sum of these two forces results in the bending force at the time of combustion. So as the engine speed increases the magnitude of the inertia force increases and this amount is deducted from the greater force which is caused by combustion, resulting in a decrease in total load magnitude. The main reason for torsional load not having much effect on the stress range is that the maximums of bending and torsional loading happen at different times during the engine cycle. In addition, when the main peak of bending takes place the magnitude of torsional load is zero.

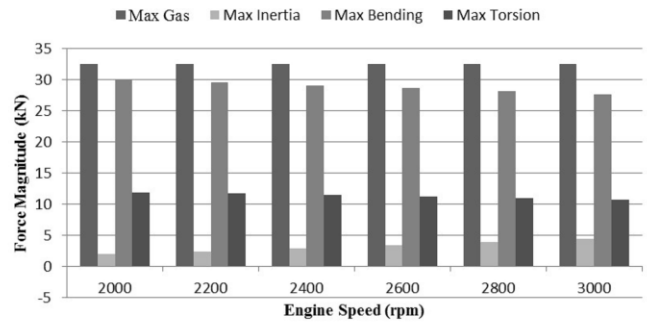

Figure 9. Comparison of maximum load between gas force, inertia, bending and torsional load at different engine speeds

The dynamic analysis of this single cylinder crankshaft is very similar to an automotive crankshaft which consists of several cylinders. The only difference is the number of applied loads to the mechanism which could be projected to the rotating plane of the crankshaft. In a multi-cylinder crankshaft the effect of combustion of other cylinders on one cylinder results in high torsional load which must be included in the analysis. Since the studied crankshaft belonged to a single cylinder engine, there would be no such effect. Therefore, the analysis could be performed without considering torsional load. The noise and vibration analysis of single cylinder and multi-cylinder crankshafts are similar. The longitudinal and radial displacements of a single throw, which consists of two main bearings, two crank webs, and a crankpin, under service load is measured in order to define the noise and vibration level of the crankshaft. Therefore, the analysis followed in this study could be implemented in the analysis of a single throw of a multi-cylinder crankshaft as well. Similar method was adopted for the dynamic analysis of crankcase. The loading in case of crankcase is proportional to that of crankshaft; hence the maximum loading in both the cases will occur at the same time. The forces acting on both the bearing ends of crankcase are calculated the shaft as a simply supported beam. Figure 10 and 11 show the forces acting on the crankcase at gearbox and flywheel end respectively. The maximum loading is caused by bending at 350^0 crank angle which is same as crankshaft. The torsional load is neglected in the same way as will be derived for crankshaft. The comparison of variation of forces on crankcase with different engine rpm is shown in Figure 12.

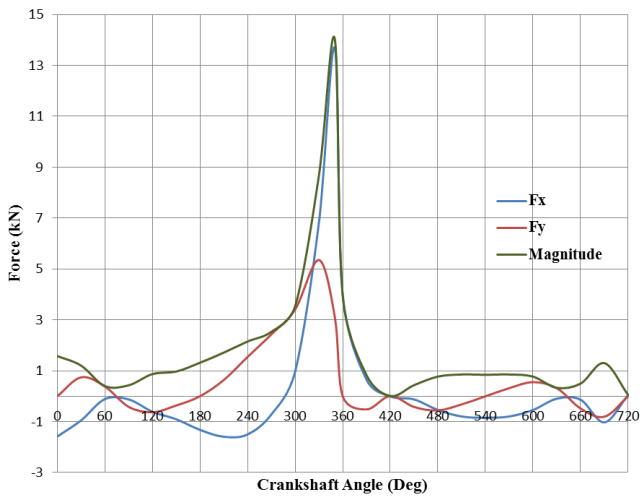

Figure 10. Variation of the force components over one complete cycle at the gearbox end of the crankcase at 2600 rpm

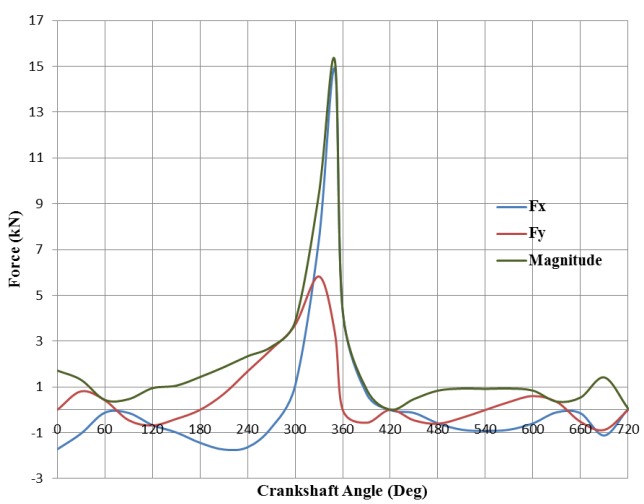

Figure 11. Variation of the force components over one complete cycle at the flywheel end of the crankcase at 2600 rpm

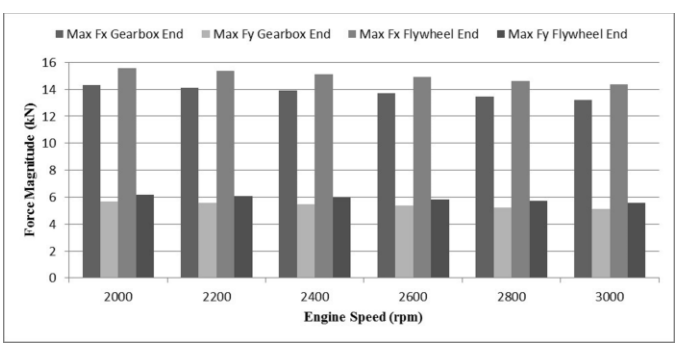

Figure 12. Comparison of maximum bending and torsional load between gearbox end and flywheel end of the crankcase at different engine speeds

IV. FEA WITH DYNAMIC LOADS

There are two different approaches for applying the loads on the crankshaft to obtain the stress time history. One method is to run the FE model many times during the engine cycle or at selected times over 720° by applying the magnitude of the load with its direction in a way that the loading could define the stress-time history of the component. Another approach to obtain stresses at different locations at different times during a cycle is by superposition of the basic loading conditions. This involves applying a unit load in the basic conditions and then scaling the stresses from each unit load according to the dynamic loading. Then similar stress components are added together. Farzin H. Montazersadgh and Ali Fatemi [4] in their paper performed analysis at 12 points over 720 degrees and the results were compared with the results from the superposition. In this paper only superposition approach was used for the engine speed of 2600 rpm to verify its results with the experimental setup. The superposition approach was used by developing a code in Excel spread sheet to perform the necessary calculation and obtain the results for the stresses at different crankshaft angles. As the dynamic loading condition was analyzed, only two main loading conditions were applied to the surface of the crankpin bearing. These two loads are perpendicular to each other. Any loading condition during the service life of the crankshaft can be obtained by scaling and combining the magnitude and direction of these two loads. The model generated for the static analysis was used for the dynamic analysis in case of crankshaft. In case of crankcase the modified model suggested to reduce the probability of crack generation was used for dynamic analysis. Proper boundary conditions and type of loading are important since they strongly affect the results of the finite element analysis. Identifying appropriate boundary conditions and loading situation are also discussed. Above mentioned FE models were used for dynamic analysis considering the boundary conditions according to the mounting of the crankshaft and crankcase in the engine.

A. *Loading and Boundary conditions*

Boundary conditions were chosen according to the actual mounting of the components in the engine. The crankshaft is constraint with a ball bearing from one side and with a journal bearing on the other side. The ball bearing is press fit to the crankshaft and does not allow the crankshaft to have any motion other than rotation about its main central axis. Since only 180 degrees of the bearing surfaces facing the load direction constraint the motion of the crankshaft, this constraint was defined as a fixed semicircular surface as wide as the ball bearing width on the crankshaft. The other side of the crankshaft is on a journal bearing. Therefore, this side was modeled as a semicircular edge facing the load at the bottom of the fillet radius fixed in a plane perpendicular to the central axis and free to move along central axis direction. Figure 13 show these defined boundary conditions in the FE model of crankshaft. For pressure P on the contact surface, the total resultant load is given by:

$$F = \int_{-\frac{\pi}{3}}^{\frac{\pi}{3}} P\,Cos\,(\varphi) rt\, d\varphi \;= P\, rt\sqrt{3} \qquad (1)$$

Where r is the crankpin radius and t is the crankpin length. As a result, the pressure constant is given by:

$$P = \frac{F}{r\,t\,\sqrt{3}} \quad (2)$$

Force F, which is the magnitude of the total force applied to the crankshaft, can be obtained from dynamic analysis at different angles. According to the geometry of the crankshaft a unit load of 1 kN will result in the pressure of 0.6598 MPa, as follows

$$P = 1000/(25 \times 35 \times \sqrt{3}) \;\; = 0.6598 \text{ MPa}$$

The engine assembly of four stroke diesel engine was used to determine the proper boundary conditions for crankcase and crankshaft. Crankcase which is the lower part of the engine is always fixed at its bottom with the bolts on the foundation. Also it can be seen that the crankshaft is constrained in a crankcase recesses with taper roller bearings at both the ends. The bearings are press fitted to the crankshaft and does not allow the crankshaft to have any motion other than rotation about its main central axis. The pressure equivalent to 1 kN were applied separately on flywheel and gearbox end of the engine. Two different load cases were created and the analysis was performed. The boundary conditions applied to the crankcase is shown in figure 13.

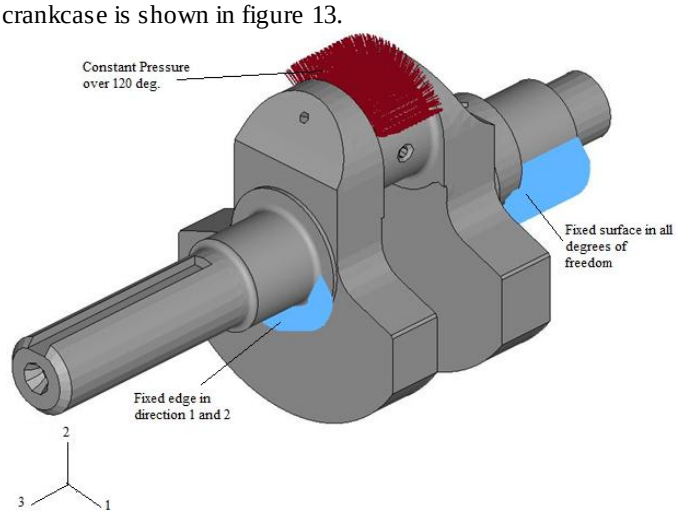

Figure 13. Boundary conditions of dynamic model of the crankshaft with the load applied on the upper part of the connecting rod bearing

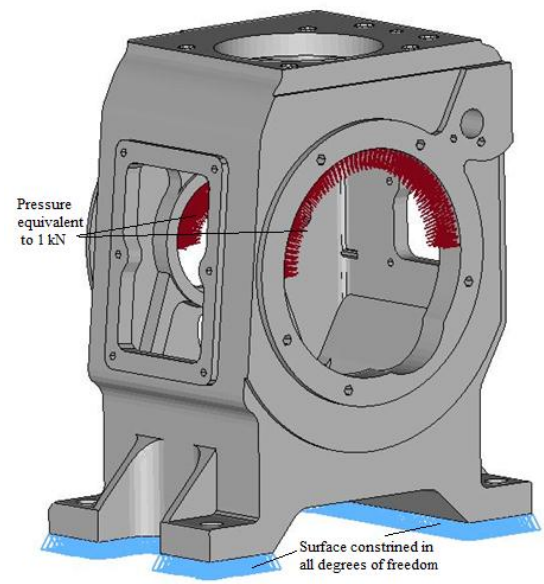

Figure 14. Boundary conditions of dynamic model of the crankcase with the load applied on the upper part of the bearing ends

V. TEST ASSEMBLY FEA

Experimental test setup was created for crankcase dynamic analysis. Strain gauges were attached to the crankcase near the previous crack position. The data of the crankcase are collected using the data acquisition system. Rosette type of strain gauges was used to calculate strain in the crankcase. Stresses were then calculated from the strain values obtained and those were compared with the results obtained from FEM. The readings were taken at the nominal engine speed which is 2600 rpm. Hence FEM results for the speed of 2600 are only considered for the comparison with the actual test values. Ease in modelling is done by using only bending load as there is very slight variation if considered with torsional load.

VI. FINITE ELEMENT ANALYSIS RESULTS AND DISCUSSIONS

The analysis conducted was based on superposition of four basic loadings in the FE analysis. The unit load applied on the connecting rod bearing was a pressure of magnitude 0.6598 MPa for crankshaft. Note that the resultant load F was 1 kN. In case of crankcase, the resultant load of 1 kN [1] was applied on both the flywheel and gearbox end. The analysis was performed separately by considering one load and the constraints for each analysis. These results from these two load steps were added to get the magnitude of stresses at different location.

Section changes in the crankshaft and crankcase geometry result in stress concentrations at intersections where different sections connect together. Although edges of these sections are filleted in order to decrease the stress level, these fillet areas are highly stressed locations over the geometry of crankcase and crankshaft. Therefore, stresses were traced over these locations.

Stress results from applying unit load on both crankshaft and crankcase are tabulated in Table 1 and Table 2. The stress components in Table 1 and 2 were used to obtain stresses at

different loading conditions by scaling these values by the magnitude of the applied load. In order to obtain stresses at any location at different crank angles these tabulated data were used as explained below:

At a crank angle for which stress components are aimed to be calculated, load components at that crank angle defined in the local rotating coordinate system are taken from the dynamic analysis with consideration of their sign. Since the analysis is based on linear elastic behavior of the material, stress magnitude has linear relation with load, therefore stresses tabulated in Tables 1 and 2 are scaled according to the proper load component. Identical stress components are then added together resulting in stress components of the aimed loading situation. Replacing these stress components in the following equation gives the von Mises stress.

$$\sigma_{\text{von Mises}} = \frac{1}{\sqrt{2}}\left((\sigma_{XX} - \sigma_{YY})^2 + (\sigma_{YY} - \sigma_{ZZ})^2 + (\sigma_{XX} - \sigma_{ZZ})^2 + 6(\sigma_{XY}^2 + \sigma_{XZ}^2 + \sigma_{YZ}^2)\right)^{1\backslash 2} \quad (3)$$

Following the above mentioned procedure, von Mises stress results for both FE models of crankcase and crankshaft were obtained.

TABLE I
STRESS COMPONENTS IN MPA AT LOCATIONS LABELED IN FIGURE 15 ON CRANKSHAFT, RESULTING FROM UNIT LOAD OF 1 KN

Location No.	S11	S22	S33	S12	S23	S13	Von Mises (Superposition)	Von Mises (FEA)
Loading Direction +Fx								
1	2.02	0.67	0.72	0.04	0.00	0.97	2.14	2.18
2	2.43	0.74	0.54	-0.08	0.00	-0.94	2.43	2.43
3	0.79	0.86	-1.72	0.39	-1.02	-3.24	6.45	8.34
4	0.94	1.75	4.42	-0.01	-0.28	-1.81	4.48	4.72
5	-1.11	-0.84	-1.11	0.82	1.48	-4.58	8.47	12.94
6	0.84	-0.80	-2.18	2.20	1.97	-0.32	5.78	7.08
7	6.98	0.29	1.49	-0.04	-0.33	2.90	7.98	8.09
Loading Direction +Fy								
1	0.14	0.01	0.03	-0.06	-0.02	0.06	0.19	0.19
2	0.14	0.01	0.03	0.21	-0.08	-0.05	0.42	0.42
3	0.22	-0.24	-0.80	-0.66	-0.28	-1.03	2.35	4.65
4	0.06	0.63	1.45	.25	-0.40	-0.48	1.68	0.84
5	0.48	0.83	0.27	-0.59	-0.42	1.20	2.47	4.02
6	1.79	0.08	2.04	0.15	-0.27	-1.84	3.73	3.73
7	-2.19	-0.13	-2.28	-0.17	0.15	2.23	4.41	4.42

A. *Finding the Critical Location*

FE analyses were performed on crankshaft and crankcase using FEA software. Investigation of the FE models shows that the fillet areas experience the highest stresses during service life of the crankshaft. Therefore, seven points on the fillets were selected and labeled in Figure 15 for crankshaft. In case of crankcase only the point near the crack initiation as shown in Figure 16 was considered as the actual testing was taken at the same location. The loading condition is the only loading condition used at the time of maximum bending load, because at this time the torsional load is zero. Therefore, using the stress results and scaling them according to the maximum dynamic load at this moment will give the maximum stress at these locations.

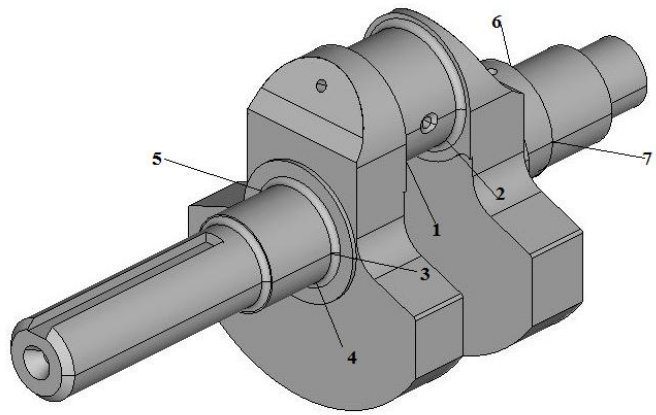

Figure 15. Locations on the crankshaft where the stress variation was traced over one complete cycle of the engine

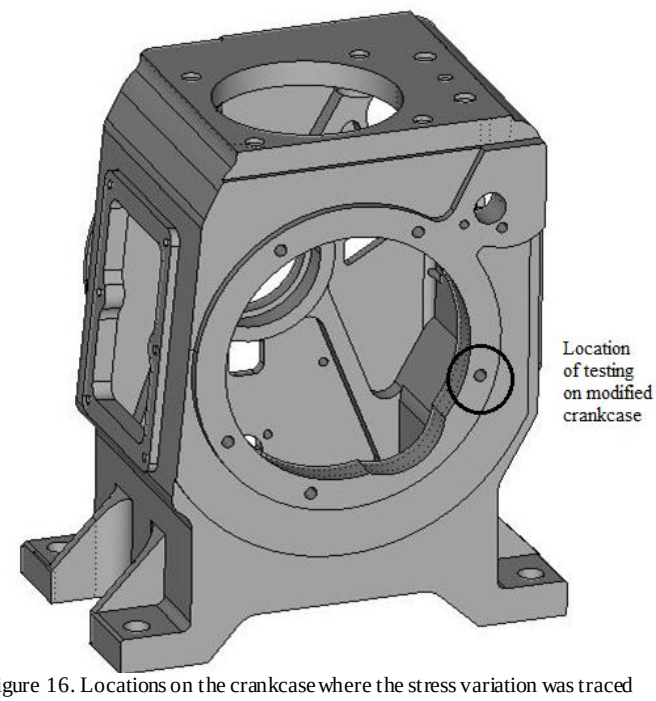

Figure 16. Locations on the crankcase where the stress variation was traced over one complete cycle of the engine

Figure 17 show the von Mises stress with sign at these seven locations at the engine speed of 2000 rpm for crankshaft. The sign of von Mises stress is same for all 7 locations on crankshaft as tension is acting on all the points as they lie below the neutral axis. Figure 18 show the von Mises stress at crack location at the engine speed from 2000 to 3000 rpm for crankcase. Engine speed of 2000 was not considered for comparison FE analysis of crankcase with experimental results as the testing was performed on its nominal operating speed of 2600 rpm. As can be seen from Figures 17, the maximum von Mises stress occurs at location 5, while other locations experience stresses lower than location 5. Therefore, other five locations were not considered to be critical in the rest of the analysis. According to the obtained results, the maximum von Mises stress value at location 5 for crankshaft is 252.94 MPa at the engine speed of 2000 rpm. As only one location was considered for the analysis of crankcase the

maximum von Mises stress obtained for this location was 61.26 and 64.01 MPa at the engine speed of 2600 rpm and 2000 rpm respectively.

Since stress range and mean stress are the main controlling parameters for calculating fatigue life of the component, these parameters have to be calculated. Figure 19 shows the minimum, maximum, mean, and range of stress at selected locations on the crankshafts at the engine speed of 2000 rpm. As can be seen from these figures, location 5 has the highest maximum stress as well as the maximum value of stress range. This location also has a positive mean stress, which has a detrimental effect on the fatigue life of the component. Therefore, location 5 is the critical location on the crankshaft, and any further discussion is with regards to this critical location on the crankshaft.

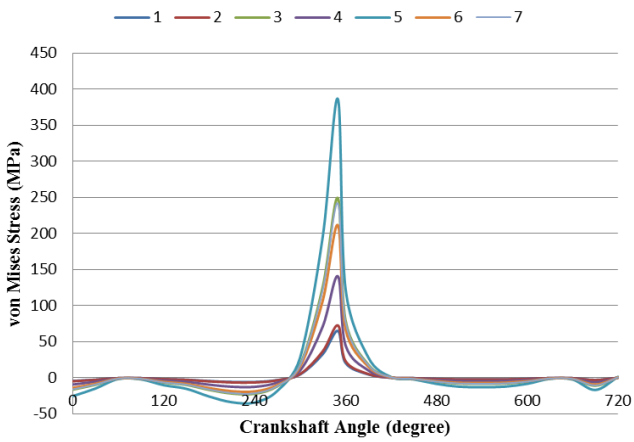

Figure 17. Von Mises stress history at different locations on the crankshaft at the engine speed of 2000 rpm

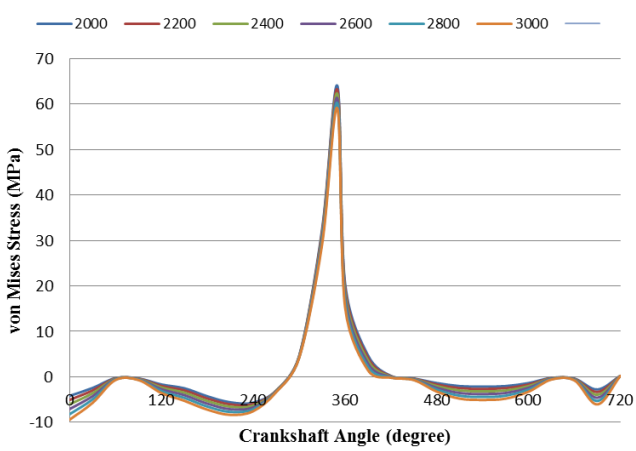

Figure 18. Von Mises stress history at crack prone location on the crankcase at different engine speeds

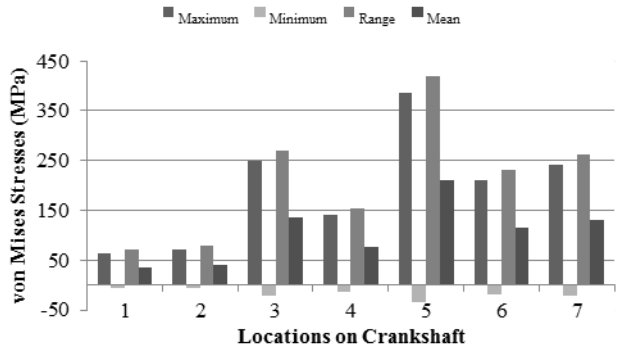

Figure 19. Comparison of maximum, minimum, mean, and range of stress at the engine speed of 2000 rpm at different locations on the crankshaft

B. *Effect of Torsional Load*

In this specific engine with its dynamic loading, it is shown that torsional load has no effect on the range of von Mises stress at the critical location. The main reason of torsional load not having any effect on the stress range is that the maxima of bending and torsional load happen at different times. In addition, when the peak of the bending load occurs, the magnitude of torsional load is zero. Therefore, crankshafts are usually tested under bending fatigue load, as it was the case for the single cylinder engine investigated in this study. Stress magnitudes without considering torsion were calculated by substituting the value of zero for all F_y load components. Figure 19 show the von Mises stresses at location 5 at the engine speed of 2000 rpm considering torsion and without considering torsion for crankshafts. It can be seen that the stress-time history remains the same with and without considering torsional load for both crankshafts. This is due to the location of the critical point which is not influenced by torsion.

C. *Validation of FEA Results with Experimental Results*

Stress results obtained from the FE model of the modified crankcase were verified by experimental component test. Rosette type strain gauges were mounted at location of crack initiation on the modified crankcase. The reason for attaching strain gages at these locations is that the previous model failed at this same location and the other critical parts are not accessible for strain gauge mounting. In addition, stress gradients in these areas are high; therefore, values measured by strain gages at these locations would not be accurate.

Dynamic strain measurement requires special type of instrumentation since oscillating frequency of the flexure is 50 Hz. This is carried out using DEWE 43V data acquisition system. It has 8 analog channels and 8 digital channels and has very high sampling rate of 200 kHz/ch. For present application, sampling rate of 5000 samples per second is selected. The DEWE 43V system is as shown in figure 22. Strain gauges are connected to analogue channels of data acquisition system by using 9-Pin connector. Quarter bridge circuit is used for the strain measurement. Since the resistance of strain gauge is 350 Ω, three fixed resistances of 350 Ω are connected in the body of 9-pin connector. The strain gauge acts as the fourth resistance completing Whetstone's bridge.

Three such connectors are made. Each is used to connect the three strain gauges in the rectangular strain gauge rosette. Figure 20 gives the setup installed for experimentation. Figure 21 shows the placement of strain gauge in the crankcase. Figure 23 show the readings taken at the actual test setup using strain gauges.

Figure 20. Experimental Setup

Figure 21. Strain Gauge Placement

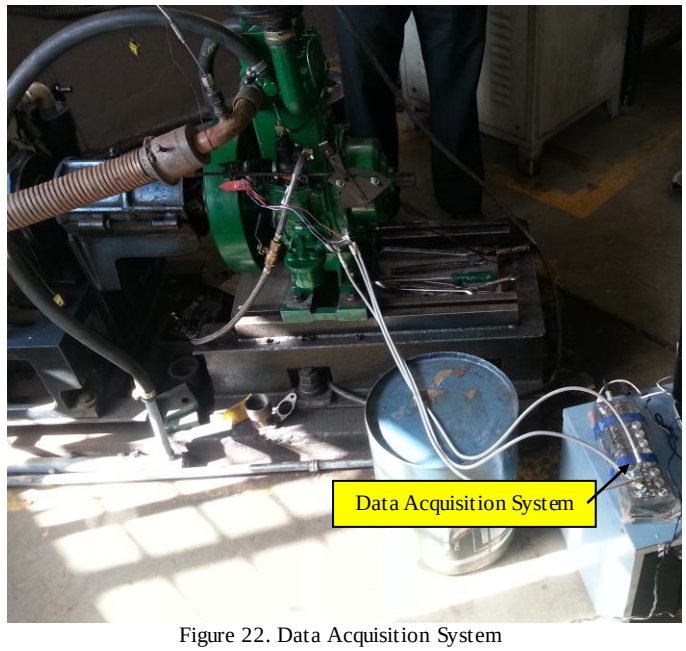

Figure 22. Data Acquisition System

The values from the strain gauges were measured when the engine was in working condition. The engine was running at 2600 rpm. The measurements from the strain gauges are tabulated in Table 3. These values were used to calculate principal stresses. The calculations of strain gauges are shown in Appendix II. The values obtained from FE analysis were compared with the experimental. Deviations from the experimental results are mentioned to prove that FE analysis is a reliable tool as well as efficient.

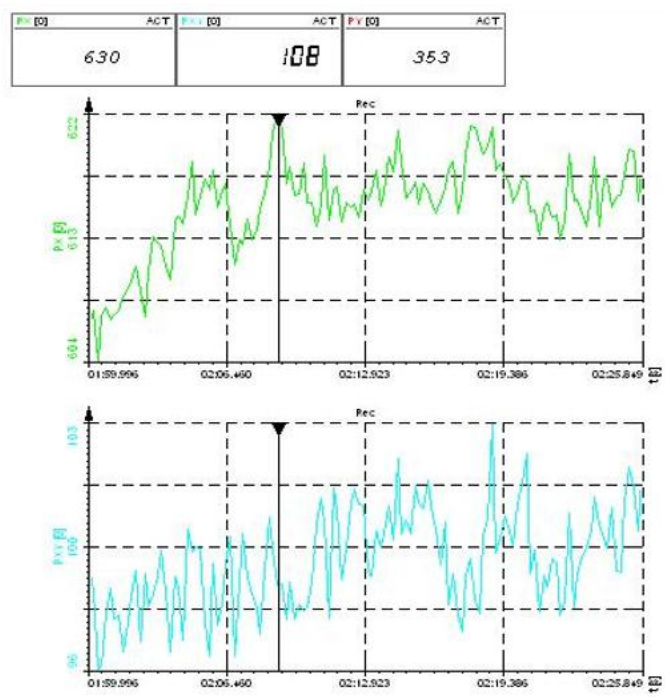

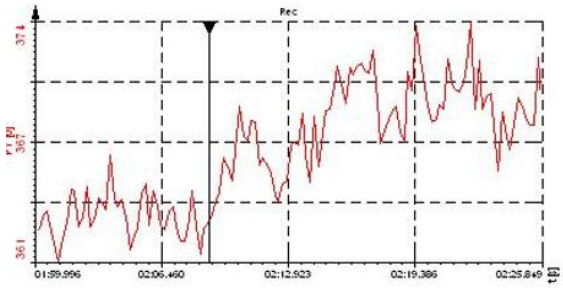

Figure 23. Readings

TABLE II
FEA STRESS RESULTS IN MPA NEAR THE PREVIOUS CRACK LOCATION OF CRANKCASE

Loading Conditions	Von Mises	Max Principal	Min Principal	Max Shear
Gearbox End	0.0796	-0.0086	-0.0892	0.0676
Flywheel End	4.0400	4.5400	0.4359	2.0600
Max Total	64.0004	70.5193	5.5072	33.0203

TABLE III
EXPERIMENTAL RESULTS

Parameters	ϵ_1 (μ strain)	ϵ_2 (μ strain)	ϵ_3 (μ strain)	Max Prin. σ_1 (MPa)	Max Shear τ_{xy} (MPa)
Experimental Results	630	108	353	78.234	24.53

TABLE IV
COMPARISON BETWEEN EXPERIMENTAL AND FEA RESULTS

Parameters	Experimental Results	FEA Results	Percentage Difference
Max Prin. σ_1 (MPa)	78.234	70.5193	9.861 %
Max Shear τ_{xy} (MPa)	24.53	21.6615	11.69%

VII. CONCLUSION

1. The plot of gas and inertial forces over one complete cycle at 2600 rpm showed the maximum force of magnitude 33.67 kN acting at crank angle of 350˚where combustion takes place, also the bi-directional force components F_x and F_y are seen to have maximum values around the same crank angle.
2. In the dynamic analysis of crankshaft superposition as well as FEA results were used for the analysis. There is vast variation between the von Mises stress obtained by superposition and that obtained by FE analysis. The reason for this variation is that the point of maximum stress occurs near the boundary conditions. FE results are unreliable at the boundary conditions and the value of location 5 was different than that of the superposition method. In this case superposition method is most reliable. The maximum stresses obtained by FEA and by superposition are 386 and 252.94 MPa respectively. Therefore it can be concluded that superposition method is more reliable for the stresses at boundary conditions.
3. Testing of crankcase was taken at one location only as it was easily accessible for mounting of strain gauges. The FE analysis was then compared with the experimental results. The comparison shows slight variation of 9.861% and 11.69% in maximum principal and shear stress respectively.
4. Thus from above analysis it can be justified that FE analysis is a reliable tool for the analysis of the component.

APPENDIX I

Gas Force:

Analytical calculation of the gas forces as a function of the angle of rotation of the crankshaft is:

$$P_G = \left[P_h \left(\frac{Sh+Sc}{Sc+Sx}\right)^n - P_{np} \right] \times A \times 10^6$$

Where,

P_h- Initial pressure of the process, (MPa)

S_h- working stroke of piston (mm)

S_c- $\frac{Sc}{\varepsilon-1}$ motion, consistent with the height of combustion chamber

P_G- Value of gas force

P_I- Inertial force of mass having linear motion

P_{RMK}- Centrifugal force caused by the mass of the connecting rods

P_{RK} - Centrifugal force generated by unbalanced mass of a crank of the crankshaft

$S_x = [(1 + 1/\lambda) - (\cos\ 〖\emptyset + 1/\lambda〗 .cos\beta)].R$

Current value of piston position (mm)

Inertia Force:

Inertial Forces of mass, having liner motion can be calculated by the following expression:

$$P_I = -M_j .\omega^2 .R\left[\frac{\cos(\phi+\beta)}{\cos\beta} + \lambda \frac{\cos_2{}^2\phi}{cos^2\beta}\right]$$

$\omega = \frac{\pi . n}{30} = \frac{\pi . 2600}{30}$ = 272.27 rad/sec – angular velocity of crankshaft

M_j = mass of particles having linear motion, [kg]

= $M_p + M_{ps}$ = 0.703 + 0.16525 = 0.86825kg

Where,

M_p = 0.703kg - the mass of piston group (piston and rings, piston pin)

M_{ps} = 0.25 x m_M = 0.16525kg - the part of mass of the rod aligned to the axis of the piston pin

m_M = 0.661kg - mass of the connecting rod

Total Force: $\Sigma P = P_G + P_I$

Bending Force: $F_x = \Sigma P \times \frac{\cos(\phi+\beta)}{\cos(\beta)}$

Torsional Force: $F_y = \Sigma P \times \frac{\sin\phi+\beta}{\cos\beta}$

APPENDIX II

Calculation for Rosette type strain gauges

Readings from the strain gauges are as follows

ε_1 = 630μ ε_2 = 180μ ε_3 = 353μ

$\varepsilon_x = \varepsilon_1$ = 630μ

$\varepsilon_y = \varepsilon_3$= 353μ

$\gamma_{xy} = 2\varepsilon_2 - (\varepsilon_1 + \varepsilon_3)$ = -623μ

$$\sigma max = \left\lfloor \frac{E}{(1-v)^2} \times \left(\varepsilon_x + v\varepsilon_y\right) \right\rfloor$$

= 78.234 MPa

$$\sigma min = \left\lfloor \frac{E}{(1-v)^2} \times \left(\varepsilon_y + v\varepsilon_x\right) \right\rfloor$$

= 19.728 MPa

$$\tau_{xy} = \left\lfloor \frac{E}{2(1-v)} \times \gamma_{xy} \right\rfloor$$

= 24.53 MPa

REFERENCES

[1] K. Sriram, R. Govindarajan, K. Nagaraja, Ravi Kharul and N. Jayaram, "Simulation of Scooter Crankcase Failure Using FEM and Dynamic Testing in Laboratory" *2003 SAE/JSAE Small Engine Technology Conference & Exhibition Madison, Wisconsin, USA* September 15-18, 2003

[2] Alexandre Schalch Mendes, Emre Kanpolat and Ralf Rauschen, "Crankcase and Crankshaft Coupled Structural Analysis Based on Hybrid Dynamic Simulation" *SAE International Journal Engines* Volume 6, Issue 4, December 2013.

[3] Hiroshi Kuribara, Junya Saito, Hidei Saito, Daisuke Sekiya, "Establishment of Prediction Technology of Fatigue Strength in Roots of Internal Thread for Crankcase Assembly and Clarification of Cracking Mechanism in Roots of Internal Thread" *SAE International Journal Engine* Volume 3, Issue 2, 28 September 2010.

Reports:

[4] Farzin H. Montazersadgh and Ali Fatemi, "Stress Analysis and Optimization of Crankshafts Subject to Dynamic Loading" , *Forging Industry Educational Research Foundation (FIERF), American Iron and Steel Institute (AISI), University of Toledo,* August 2007

[5] Radoslav P., "Design a four-cylinder Internal Combustion Engine", *Project and Engineering Department, Pamplona,* 27 June 2011.